Acid-Catalyzed Polycondensation of Furfuryl Alcohol: Mechanisms of Chromophore Formation and Cross-Linking

Mekki Choura, Naceur M. Belgacem, and Alessandro Gandini*

Matériaux Polymères, Ecole Française de Papeterie et des Industries Graphiques (INPG), BP 65, 38402 Saint Martin d'Hères, France

Received October 12, 1995; Revised Manuscript Received January 22, 1996[⊗]

ABSTRACT: A thorough investigation of the acid-catalyzed polycondensation of furfuryl alcohol was conducted with the specific aim of understanding the mechanisms responsible for the main reaction, but more particularly for the transformation of linear unconjugated oligomers into black cross-linked final materials. The originality of the present approach, compared with previous unsuccessful attempts, consisted in calling upon numerous model compounds simulating specific features of both the monomer and its condensation products. The formation of conjugated sequences along the poly(furfuryl) chains is caused by repetitive cycles involving the loss of hydride ions followed by the deprotonation of the carbenium ions thus formed. This reaction was simulated and accelerated by using cationic hydride-ion abstractors. The branching reactions only occur after the appearance of the multiple unsaturations and owe their origin to interchain cycloadditions between furan rings and conjugated structures. A long-standing puzzle has thus been solved.

Introduction

Apart from its obvious interest as energy feedstock, the vegetal biomass constitutes an enormous renewable source of different monomers (monosaccharides, terpenes, alcohols, etc.), oligomers (rosins, drying oils, tannins, hemicelluloses, etc.), and polymers (cellulose, starch, lignins, etc.).[1,2] Our laboratory has been working for many years on the valorization of these resources in order to elaborate novel polymeric materials possessing a variety of potential applications. The strategy behind this approach stems from the following basic considerations: (i) the raw materials are available everywhere, albeit in specific vegetal species according to geographical location; (ii) they are constantly regenerated by photosynthesis; and (iii) they can provide original polymeric structures not readily available via petroleum-based chemistry. Furanic monomers constitute a typical example of this strategy, and we have investigated widely their synthesis, polymerization, and the characterization of the ensuing macromolecules.[1−3] The presence of this heterocycle within the main chain or as a side function in polymeric structures can provide original and valuable properties such as high-strength fibers,[4] polyurethane foams and elastomers,[5,6] and conjugated polymers.[7]

Two first-generation furanic derivatives can be readily obtained from saccharidic sources, ubiquitous in nature in the form of monomers, oligomers, and polymers: furfural from pentoses and (hydroxymethyl)furfural from hexoses. These two compounds have been used as the starting point for the syntheses of a large family of furanic monomers adapted to chain or step polymerization reactions. At present however, the vast majority of furfural is converted industrially into furfuryl alcohol (FA), because the materials derived from the latter have found a useful range of applications, mostly for foundry cores and molds, corrosion-resistant materials, and precursors to graphitic composition and adhesives.[8,9] Thus, furfuryl alcohol is still the most important furanic derivative on the market.

All the resins derived from FA call upon the action of an acidic catalyst which promotes a complex polycondensation process leading to black cross-linked materials. According to the specific conditions used, mostly the type and strength of the acid, the presence of water, and the temperature, the kinetics of this process can vary considerably and thus be adapted to the delay requirements of the specific application.[8,9] Surprisingly, despite much research work published over the last 30 years,[1−3,8−25] the detailed mechanisms responsible for the progressive coloration and the branching of these polymers are not well understood.

There is a general consensus today about the fact that the main acid-catalyzed reaction in the resinification of FA is in accordance with the very first hypothesis put forward by Dunlop and Peters,[26] who proposed two alternative mechanisms (Scheme 1) consisting of either the condensation of the OH group with the mobile hydrogen atom of the heterocycle at C5 to give structure **1**, or the much less frequent OH−OH condensation to give occasional CH_2OCH_2 linkages as in structure **2**. The fact that the latter moieties are in a minority is moreover ascribed to their acid-catalyzed loss of formaldehyde which generates structure **1**, as indicated in the reaction Scheme 1. However, only oligomers of DP up to 5 have been isolated and characterized unambiguously, and these include exclusively *linear* structures containing either or both intercycle bridges, viz., methylene and dimethylene ether moieties joined by C2−C5 furan rings.[22,23]

These simple pathways and the resulting structures predict only linear macromolecules without any chromophore, and therefore the ensuing materials ought to be colorless (2,5-dimethylfuran absorbs at 220 nm) thermoplastic polycondensates. As pointed out above, the results are completely different in that without exception these systems develop an intense color during the polymerization and yield gelled materials which after neutralization and drying are blackish insoluble powders. It is therefore obvious that other reactions must accompany the two condensation steps shown in Scheme 1 and that these "side" events must occur whatever the experimental conditions (type and strength of acid, temperature, solvent) and be more important than occasional diversions from the expected linear growth.

* Author to whom correspondence should be addressed. Phone: 00-33-76-82-69-47. E-mail: Alessandro.Gandini@efpg.grenet.fr.

[⊗] Abstract published in *Advance ACS Abstracts,* April 1, 1996.

S0024-9297(95)01522-1 CCC: $12.00

Scheme 1

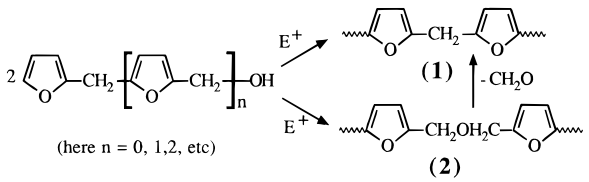

The blatant contradiction between the simple polycondensation Scheme 1 and the actual phenomenology has of course puzzled researchers in the past, and many attempts to unravel these problems have been published together with proposals of specific mechanisms. Wewerka et al.[13,14] and Milkovic et al.[15] suggested a reaction between the hydrogen atoms at C3 and C4 of furan moieties with the formaldehyde formed in the polycondensation followed by cross-linking between the primary OH thus formed and a hydrogen atom at C5. Conley and Metil[16] and Maciel et al.[17] interpreted their IR and ^{13}C-NMR spectra of FA resins as proof that the hydrogen atoms at the C3 and C4 positions are not involved in branching (cross-linking) reactions. They proposed as an alternative that these ramifications arise from the methylene bridges between two furan rings, but the supporting evidence they provided was unconvincing. Glowinski and Pajak[18] detected paramagnetic centers in FA resins which suggested the presence of highly conjugated structures, but did not offer any mechanistic justification for their formation. Finally, Buchwalter[21] used furfuryl acetate as a model compound for resinification and obtained essentially the same results as with FA. He was mostly concerned with the mechanism responsible for color formation and proposed, on the basis of spectroscopic evidence, a mechanism similar to that given by Gandini et al.[27,28] for an analogous phenomenon in the cationic polymerization of 2-alkenylfurans.

In conclusion, despite serious attempts at unravelling the origin of color and cross-linking in the acid-catalyzed polycondensation of FA, no clear-cut answer was available concerning either mechanism. We decided to take up the challenge, but proceeded in a different way, namely, using model compounds to simulate certain specific features of the monomer and the oligomers.

Experimental Section

Model Compounds. Commercial Model Compounds. FA, furan (F), 2-methylfuran (MF), 2,5-dimethylfuran (MMF), 3,4-dihydrofuran, 2,5-dimethoxy-3,4-dihydrofuran, isoprene, and furfuryl mercaptan (FM) were commercial products, purified by distillation and dried over calcium hydride. 2,5-Bis(hydroxymethyl)furan (BHMF) was a kind gift from QO Chemicals Europe and was purified by recrystallization from chloroform or by vacuum sublimation: the latter technique provided a product of higher purity, mp 70 °C.

Synthesis of Monomeric Model Compounds. 5-Methylfurfuryl alcohol (MFA), 1-(2-furyl)-1-ethanol (FE1), 2-(2-furyl)-2-propanol (FP), and 2-(2-furyl)-1-ethanol (FE2) were prepared following the procedures described elsewhere.[29−31] The fluorinated alcohols, namely, 1,1,1-trifluoro-2-(2-furyl)-2-propanol (TMFP), bp 50 °C/15 torr, and 1,1,1-trifluoro-3,3,3-trifluoro-2-(2-furyl)-2-propanol (TFFP), bp 200 °C, were prepared in 60−70% yields by the classical condensation of 2-furyllitium with ketones, here trifluoroacetone and hexafluoroacetone, respectively.

Trimethyloxy-2-furfurylsilane (FAS), bp 80 °C/15 torr, trimethyloxy-2-isopropylfurylsilane (FPS), and trimethyloxy-5-methyl-(2-furfuryl)silane (MFAS) were obtained in 70% yields by the corresponding reactions of FA, FP, and MFA with trimethylchlorosilane at room temperature using triethylamine as catalyst. 2-Furfuryl acetate (FAC), bp 90 °C/32 torr, and 5-methyl-(2-furfuryl) acetate (MFAC) were synthesized in 80% yields by the esterification reactions of FA and MFA, respectively, with acetic anhydride in the presence of potassium carbonate. 2-(Hydroxyacetyl)furan (HAF) was prepared from 2-furoyl chloride and *N*-methyl-*N*-nitroso-*p*-toluenesulfonamide as a source of diazomethane as previouly reported.[32] 2,2-(2-Furyl)propane was synthesized to be used as an intermediate for the preparation of 5-(hydroxymethyl)-2,2-bis(2-furyl)propane (HMFP). It was obtained by the classical condensation of two molecules of furan with acetone in aqueous HCl. Its monolithiation and subsequent reaction with formaldehyde gave HMFP in 45% yield, bp 120 °C/10^{-2} torr.

All the above compounds were characterized by FTIR and ^{1}H-NMR spectroscopy. The IR spectra were entirely consistent with the expected structures, which were clearly corroborated by the NMR spectra as shown by the data in Table 1.

Synthesis of Oligomeric Model Compounds. To our knowledge, bis[2-(5-methylfuryl)]methane (BMFM), bis[2-(5-methylfuryl)]ethane (BMFE), and bis[2-(5-methylfuryl)]propane (BMFP) have never been reported in the literature, except for a mention to BMFE.[28] BMFM was prepared in hexane from 2 mol of MF and 1 mol of trioxane in the presence of Lewatit resin as an acidic catalyst. The reaction was carried out for 1 h at 50 °C and gave 50% of BMFM which was purified by distillation (bp 93 °C/7 torr). BMFE and BMFP were prepared in bulk by the HCl-catalyzed condensation of 2 mol of MF with 1 mol of acetaldehyde and acetone, respectively, at 0 °C and purified by distillation (bp 95 °C/7 torr for BMFE and 100 °C/7 torr for BMFP). The reaction yields were 60% for BMFE and 85% for BMFP. 2,5-Bis(2,5-methylfurfuryl)-furan (BMFF) was obtained by the analogous reaction of 2 mol of MF with 1 mol of BHMF with $TiCl_4$ as catalyst and purified by vacuum removal of solvent and residual reagents and recrystallization from hexane (mp 34 °C). The reaction yield was only 5% because of important resinification reactions.

The oligomeric model compounds were characterized by FTIR and ^{1}H- and ^{13}C-NMR spectroscopy. The IR spectra were entirely consistent with the expected structures, and the NMR data, shown in Table 2, confirmed this.

Other Reagents and Solvents. The dioxolenium salts 1-isopropyl-4,5-dimethyldioxolenium hexachloroantimonate (IDDCA) and hexafluoroarsenate (IDDFA) were kindly offered by Prof. Zedlinski of the Polish Academy of Sciences, Zabrze. The other reagents and solvents used in this investigation were commercial products used as such or after adequate purification.

Polymerization Systems. General Procedure. Reactions leading to polymer formation were carried out under nitrogen by mixing the monomer (or the two monomers in the case of copolymerization systems) with solvent. The temperature was kept at the desired constant value by a thermostated bath, and the catalyst was added under vigorous stirring using a microsyringe. At the end of the reaction, the mixture was neutralized by adding an aqueous ammonia solution. The organic phase was then extracted with dichloromethane, washed with water, and dried with sodium sulfate. The resulting product was finally isolated by solvent removal under vacuum. These products will be called "polymers" in this paper, even if their DPs were often low.

Polymer Characterization. Polymers were characterized by UV, NMR, and FTIR spectroscopy, vapor pressure osmometry (VPO), GPC, and DSC. The chromatograms were recorded on a Knauer GPC equipped with 4 Styragel columns (100, 500, 1000, and 10 000 Å) connected in series and two detectors: a UV sensor working at 254 nm and a refractometer. The calibration curve was obtained using standard polystyrene samples.

Results and Discussion

The two different aspects relevant to this study, viz., the cross-linking and color-forming mechanisms, will be discussed concomitantly because they bear much in common.

Table 1. Chemical Structures of the Monomeric Model Compounds Used in This Work and Their ^{1}H-NMR Characteristics (300 MHz, CD_2Cl_2, TMS)

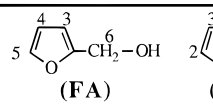 **(FA)**	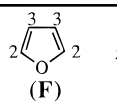 **(F)**	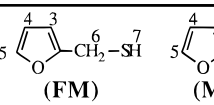 **(FM)**	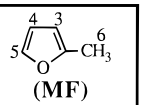 **(MF)**
H^3 and H^4 = 6.3; H^5 = 7.4; H^6 = 4.5; OH = 3.5.	H^3 = 6.3; H^2 = 7.4	H^3 and H^4= 6.2-6.4; H^5 = 7.4; H^6 = 3.8; SH = 1.9.	H^3 and H^4 = 6.3 H^5 = 7.4; H^6 = 2.2.
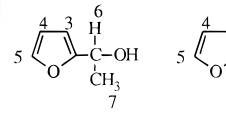 **(FE1)**	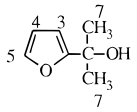 **(FP)**	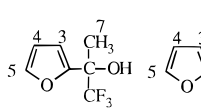 **(TMFP)**	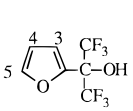 **(TFFP)**
H^3 and H^4= 6.2; H^5 = 7.2; H^6 = 4.7; H^7 = 1.4; OH = 3.1.	H^3 and H^4 = 6.2; H^5 = 7.3; H^7 = 1.5; OH = 3.2.	H^3 and H^4= 6.3; H^5 = 7.4; H^7 = 1.7; OH = 3.2.	H^3 and H^4 = 6.6; H^5 = 7.7; OH = 5.1.
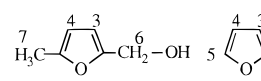 **(MFA)**	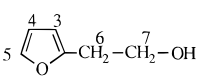 **(FE2)**	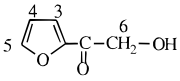 **(HAF)**	
H^3 = 6.1; H^4 = 5.9; H^6 = 4.5; H^7 = 2.3; OH = 3.1.	H^3 = 6.2; H^4 = 6.0; H^5 = 7.2; H^6 = 3.8; H^7 = 2.9; OH = 3.7.	H^3 = 7.4; H^4 = 6.7; H^5 = 7.2; H^6 = 4.8; OH = 3.1.	
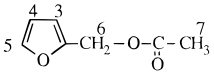 **(FAC)**	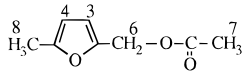 **(MFAC)**		
H^3 and H^4= 6.2-6.3; H^5 = 7.3; H^6 = 4.5; H^7 = 2.1.	H^3 and H^4= 6.2-6.3 H^6 = 4.5; H^7 = 2.1; H^8 = 2.3.		
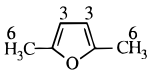 **(MMF)**	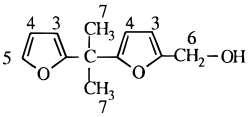 **(HMFP)**		
H^3 = 5.8; H^6 = 2.2;	H^3 and H^4= 6.0-6.3; H^5 = 7.3; H^6 = 4.4 H^7 = 1.6; OH = 2.3.		
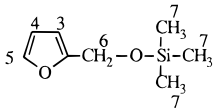 **(FAS)**	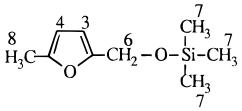 **(MFAS)**		
H^3 and H^4= 6.2-6.3; H^5 = 7.3; H^6 = 4.5; H^7 = 0.15.	H^3 and H^4= 6.2-6.3; H^6 = 4.5; H^7 = 0.15; H^8 = 2.3.		
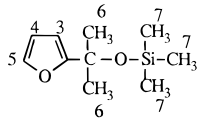 **(FPS)**			
H^3 and H^4= 6.2; H^5 = 7.3; H^6 = 1.5; H^7 = 0.15.			

Table 2. Chemical Structures of the Oligomeric Model Compounds Used in This Work and Their ^{1}H- (300 MHz) and ^{13}C-NMR Characteristics (CD_2Cl_2, TMS)

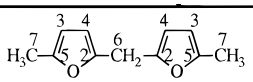 **(BMFM)**	
H^3 and H^4= 5.85; H^5 = 2.20; H^6 = 3.85. C^2 and C^5 = 149.9-150.6; C^6 = 27.3; C^3 and C^4 = 106.0-106.7; C^7 = 13.1.	
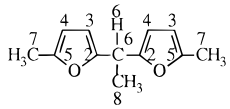 **(BMFE)**	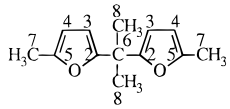 **(BMFP)**
H^3 and H^4= 5.86; H^7 = 1.50-1.56; H^6 = 4.07; H^8 = 2.20; C^2 = 150.5; C^5 = 155.0; C^6 = 33.2; C^3 and C^4 = 105.4-105.9; C^7 = 18.1; C^8 = 13.3.	H^3 and H^4 = 5.84; H^7 = 2.21; H^8 = 1.58. C^2 = 150.1; C^5 = 158.3; C^6 = 37.0; C^3 and C^4 = 104.3-105.5; C^8 = 28.2; C^7 = 13.2.
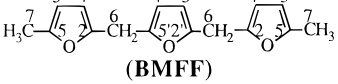 **(BMFF)**	
H^3 and H^4= 5.84-5.91; $H^{3'}$ and $H^{4'}$= 5.95; H^5 = 2.23; H^6 = 3.83. C^7 = 13.3; C^6 = 27.5; C^3 = 106.1; C^4, $C^{3'}$ and $C^{4'}$ = 107.0; C^2 = 149.8; C^5 = 150.7; $C^{2'}$ and $C^{5'}$ = 150.8.	
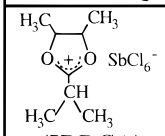 **(IDDCA)**	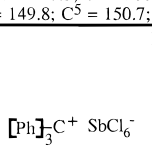 **(IDDFA)**
 **(TAA)**	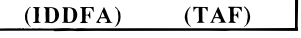 **(TAF)**

Table 3. Acid-Catalyzed Homopolymerization Conditions of FA in Dichloromethane

polymer no.	$[FA]_0$ (mol/L)	catalyst	$[C]_0 \times 10^2$ (mol/L)	T (°C)	t (h)	yield (%)	product viscosity (mPa·s)
I	1	$SnCl_4$	2	0	24	<1	25
II	3	$SnCl_4$	2	0	6	5	345
III	5	$SnCl_4$	2	0	6	11	69
IV	5	$SnCl_4$	2	10	6	20	34
V	5	$TiCl_4$	2	25	6	30	207
VI	5	$TiCl_4$	2	25	6	35	1940
VII	5	$TiCl_4$	1	25	6	29	1650
VIII	5	$TiCl_4$	4	25	6	42	2140
IX	5	$TiCl_4$	4	0	6	27	

First the acid-catalyzed homo- and co-polymerizations of the FA model compounds in bulk and in CH_2Cl_2 solution will be examined. The following systems were investigated: (1) homopolymerization, FA, FAS, MFA, MFAS, MFAC, FE1, FP, FAS, HMFP, FE2, TMFP, TFFP, HAF, FM; (2) copolymerization, FA/FAS, FAS/FPS.

Later the discussion will move onto the hydride-ion mobility both of the four model compounds simulating the oligomers and of samples of polyFA itself, studied by UV and NMR spectroscopy in the presence of hydride-ion abstractors.

Homopolymerization Systems. Polymerizations in CH_2Cl_2. First of all, the polycondensation of FA was studied using Lewis-acid catalysis under mild conditions in order to avoid cross-linking. Table 3 gives these conditions as well as the polymer yields and the final viscosity of each isolated product. These data show unsurprisingly that the increase in monomer and catalyst concentration and a rise in reaction temperature induced a corresponding increase in the polymer viscosity and yield. A typical example of thorough characterization is provided here for polymer IX. Its FTIR spectrum, given in Figure 1, showed important differences with respect to that of FA, namely, (i) a substantial decrease of the νOH band around 3450 cm^{-1}; (ii) the presence of a band at 793 cm^{-1} characteristic of 2,5-disubstituted furan rings; (iii) a weak band around 2980 cm^{-1} suggesting the presence of methyl groups; and (iv) a weak carbonyl band at 1715 cm^{-1} suggesting the occurrence of some ring-opening, probably induced by the acidic medium in the presence of the accumulated condensation water. Reactions catalyzed by various Brönsted acids gave the same qualitative features.

From the ^{1}H-NMR spectrum of polymer IX, shown in Figure 2, DP_n can be obtained alternatively from one of

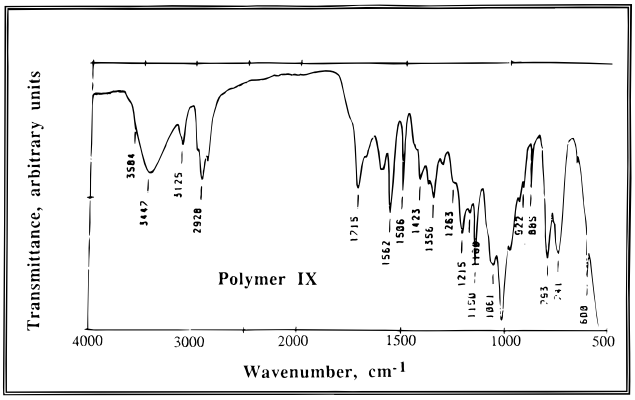

Figure 1. FT-IR spectrum (liquid film) of polymer IX.

the following relationships (eq 1), if it is assumed that **1** is the dominant structure.

$$DP_n = \frac{I_{3,4}}{2I_5} = \frac{I_{CH_2}}{I_{CH_2OH}} \quad (1)$$

Here each I_i is the value of the resonance intensity of the given i proton(s). The results of these calculations are given in Table 4 which also collects the values of M_n, M_w, and I_p obtained from GPC and those of M_n obtained from VPO. The corresponding DP_n values were calculated assuming structure **1**. Some other relevant intensity ratios extracted from the NMR spectrum in Figure 2 complete the data of Table 4.

Some important remarks can be drawn from these values: (i) The DP_n values calculated using relationships 1 are very close (2.6 and 2.5), which confirms that the incidence of CH_2-O-CH_2 bridges can be neglected. (ii) The substantial difference between the values of DP_n calculated from the NMR spectrum (2.6 and 2.5) and those obtained from GPC and VPO measurements (5.8 and 5.1, respectively) reveals that the structure of polymer IX cannot be linear. (iii) Further evidence corroborates the conclusion drawn in point (ii). In fact, in the case of linear structure **1**, the following relationship should be verified:

$$\frac{I_{OH}}{I_5} = \frac{I_{CH_2}}{I_{3,4}} = 1 \quad (2)$$

However, for polymer IX, these ratios are equal to 0.5 and 0.6, respectively (see Table 4). (iv) The high experimental DPs compared with the calculated values, coupled with the fact that ratios in eq 2 are less than unity, suggest that the structure of polymer IX is branched and that the branching reaction must involve the CH_2 groups and not the C3/C4 sites.

Another important observation is a signal at 2.2 ppm which suggests the presence of methyl groups attached to the C2 or C5 position of the furan ring. This is not new since methylated FA oligomers have been isolated and characterized previously.[22,23]

The behavior of furfuryl acetate (FAC) was entirely similar to that of FA, as already reported by Buchwalter,[21] which indicates that the presence of water accumulating during the polycondensation of the latter does not alter the qualitative features of these systems compared to acetic acid which is the condensation product arising from the former.

The reaction conditions and the polymer yields of FA model compounds are presented in Table 5. The sys-

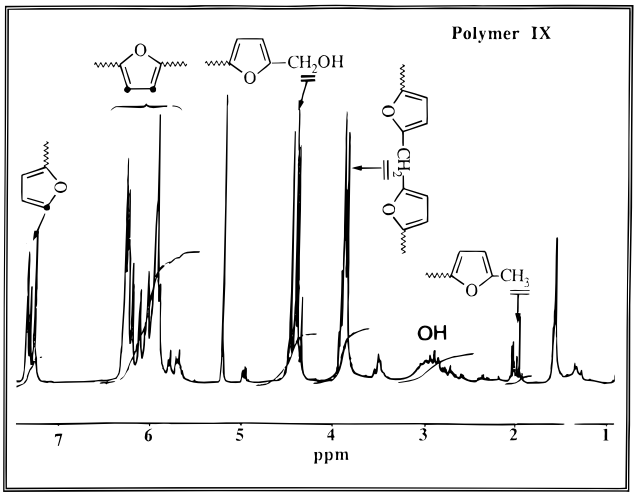

Figure 2. ^{1}H-NMR spectrum (300 MHz) of polymer IX in CD_2Cl_2.

tems involving FAS with three different Lewis acids in a dry organic medium showed that this silylated compound did not react with itself and its inertness under these conditions extended to several days as confirmed by taking NMR spectra of these solutions prepared directly in a sample tube. This observation confirms, if needed, that the presence of OH groups is essential to the polycondensation of FA. Indeed, if aqueous solutions of Brönsted acids were used as catalysts or small amounts of water were added to the dry Lewis-acid systems, FAS gave polymers with very similar structure and DP as those obtained with FA as discussed above, albeit at lower rates. This is certainly due to the progressive hydrolysis of the silyl groups which regenerates the OH groups. The small amount of FA initially formed condenses with the C5 positions of both FAS and other molecules of itself, and the water arising from these reactions hydrolyzes further FAS etc. As expected, it was found that the lower the water initially added to the dry system, the slower the polycondensation.

The acid-catalyzed reaction involving MFA (Table 5) gave a high yield of BMFM. The formation of this product can be explained by invoking a head-to-head reaction as in Scheme 1, followed by the loss of formaldehyde, as shown in Scheme 2.

Both the silylated derivative MFAS and the acetate MFAC were totally inert to the presence of a Lewis acid in dry methylene chloride, as verified by NMR analyses extended over periods of days.

The system involving FE1 yielded a dark viscous polymer (XVII) with an FTIR spectrum showing bands which suggested condensation reactions similar to those encountered with FA and a weak peak at 1715 cm^{-1} indicating some ring opening. The major difference here was kinetic, since under identical mild conditions (Tables 3 and 5), this polycondensation was much slower than that of FA. Both FA and FE1 gave insoluble solid materials when treated under more severe conditions, but again the latter took much longer to crosslink.

These results pointed to a possible key role played by methyl substitution and encouraged us therefore to try FP. Indeed, this system gave a qualitatively different behavior, since the product was now a colorless soluble polymer (XVIII) obtained in high yields (Table 5). The FTIR spectrum of XVIII (Figure 3) was consistent with a regular structure and again showed weak

Table 4. M_n, M_w, I_p, DP, and Different Calculations from the ^{1}H-NMR Spectra of Some Polymers

	GPC				VPO[a]		DP$_n$ by NMR		integral ratios	
polymer no.	M_n	M_w	I_p	DP$_n$	M_n	DP$_n$	$I_{3,4}/2I_5$	I_{CH_2}/I_{CH_2OH}	I_{OH}/I_5	$I_{CH_2}/I_{3,4}$
IX	460	1700	3.7	5.8	410	5.1	2.6	2.5	0.5 (1)[b]	0.6 (1)[b]
XVIII	610	1188	1.95	5.6	580	5.3	5.0	4.6[c]	1.0 (1)[b]	
XIX	1250	2413	1.93	11.5	1150	10.5	10.0	9.7[c]	1.0 (1)[b]	
XX					930	4.9	2.0[d]	2.0[c]	1.6[e] (4)[b]	0.12[f] (0.33)[b]

[a] VPO: vapor pressure osmometry. [b] Values in parentheses are theoretical values based on linear head-to-tail structures. [c] $I_{CH_3}/6I_5$. [d] $I_{3,4}/4I_5$. [e] I_{CH_2}/I_5. [f] I_{CH_2}/I_{CH_3}.

Table 5. Acid-Catalyzed Homopolymerization Conditions and Yields of Different Model Compounds in Dichloromethane

polymer no.	monomer	[M]$_0$ (mol/L)	catalyst	[C]$_0 \times 10^2$ (mol/L)	T (°C)	t (h)	yield (%)
X	FAS	5	$TiCl_4$	5	25	24	0
XI	FAS	5	$SnCl_4$	5	25	24	0
XII	FAS	5	$ZnCl_2$	5	25	24	0
XIII	MFA	5	$TiCl_4$	5	25	24	70
XIV	FAC	5	$SnCl_4$	2	20	24	100
XV	MFAC	5	$SnCl_4$	2	20	100	0
XVI	MFAS	5	$SnCl_4$	2	20	100	0
XVII	FE1	5	$SnCl_4$	2	20	100	80
XVIII	FP	5	$TiCl_4$	2	25	24	80
XIX	FPS	5	$TiCl_4$	2	25	24	90
XX	HMFP	5	$TiCl_4$	2	25	24	90
XXIa	TMFP	5	$TiCl_4$	5	25	24	0
XXIb	TMFP	5	$SnCl_4$	5	25	24	0
XXIIa	TFFP	5	$TiCl_4$	5	25	24	0
XXIIb	TFFP	5	$SnCl_4$	5	25	24	0
XXIII	FE2	5	$TiCl_4$	5	25	3 weeks	60
XXIV	HAF	5	$TiCl_4$	5	25	24	90
XXV	FM	5	$TiCl_4$	5	25	24	80

Scheme 2

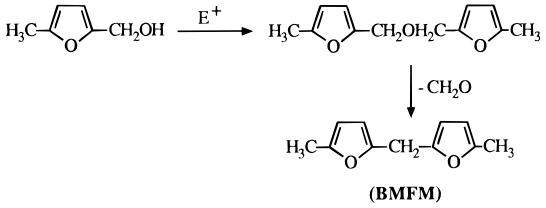

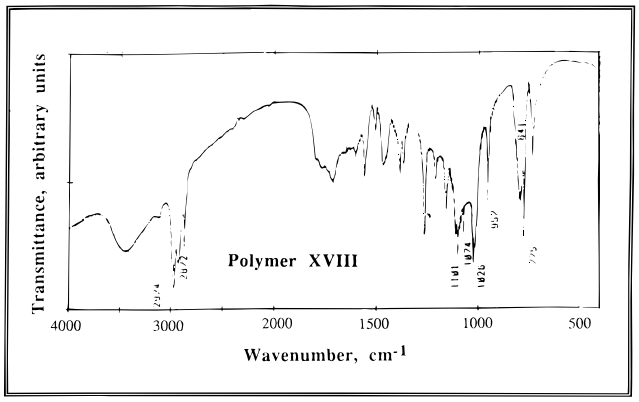

Figure 3. FT-IR spectrum (liquid film) of polymer XVIII.

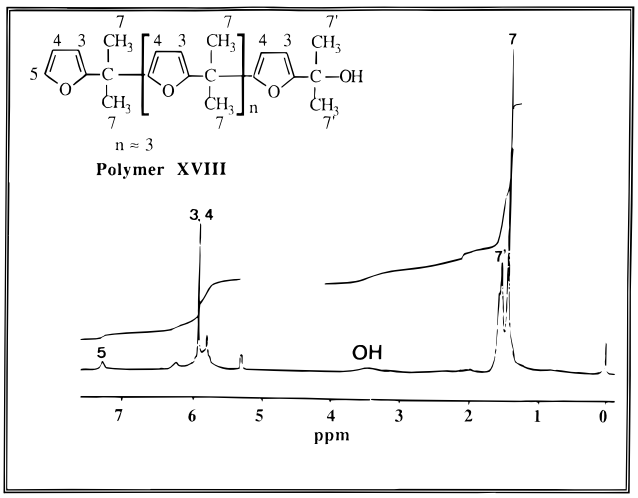

Figure 4. ^{1}H-NMR spectrum (300 MHz) of polymer XVIII in CD_2Cl_2.

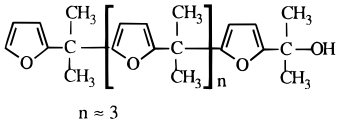

polymer XVIII

carbonyl bands attributed to sporadic acid-catalyzed hydrolytic ring opening. The simple linear structure of XVIII was clearly confirmed by its ^{1}H-NMR spectrum (Figure 4) where one encounters the relevant peaks attributed to the expected unit, in the right intensity ratio, and the resonances of the OH and H5 end groups. The DP$_n$ values determined by GPC and VPO were this time in good agreement with those obtained from the appropriate intensity ratios of NMR peaks, as shown in Table 4. These results prove that polymer XVIII possessed the following structure arising from head-to-tail condensation reactions, without side events (except from sporadic ring opening):

Thus, branching reactions could be eliminated by replacing the hydrogen atoms on the carbon atom bearing the OH function by methyl groups.

Although different experimental conditions, such as monomer and catalyst concentration, temperature, and reaction time, were tested in order to increase the DP of XVIII, it never exceeded about 6. This is ascribed to the accumulation of moisture in the system which inhibited further condensation. To avoid this drawback, we prepared the silylated derivative, FPS, which was then polymerized in the same conditions as FP, but in the presence of 2% of the latter in order to initiate the

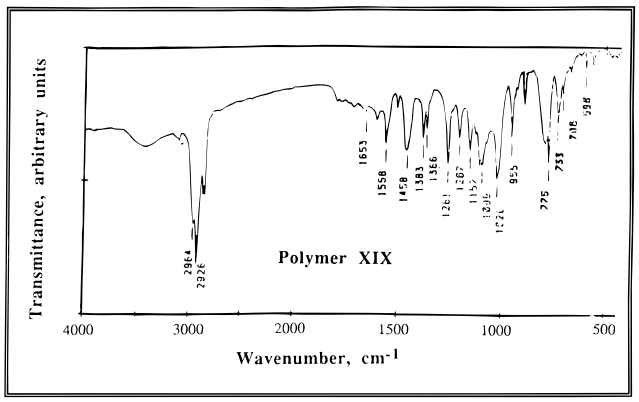

Figure 5. FT-IR spectrum (liquid film) of polymer XIX.

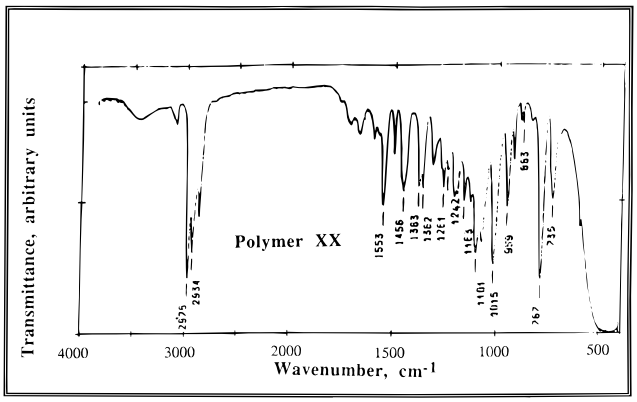

Figure 7. FT-IR spectrum (liquid film) of polymer XX.

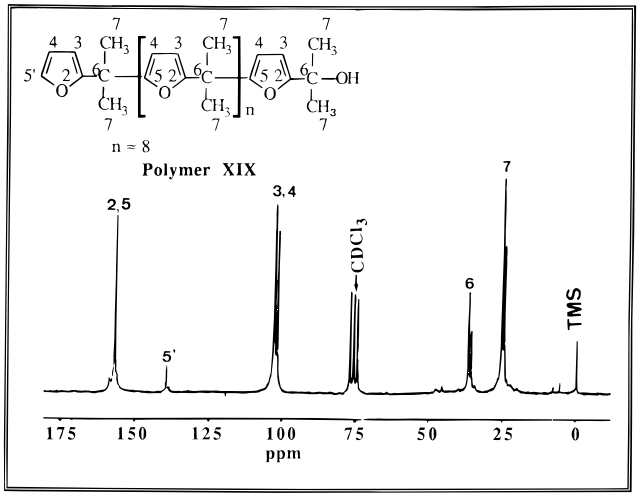

Figure 6. ^{13}C-NMR spectrum (75 MHz) of polymer XIX in $CDCl_3$.

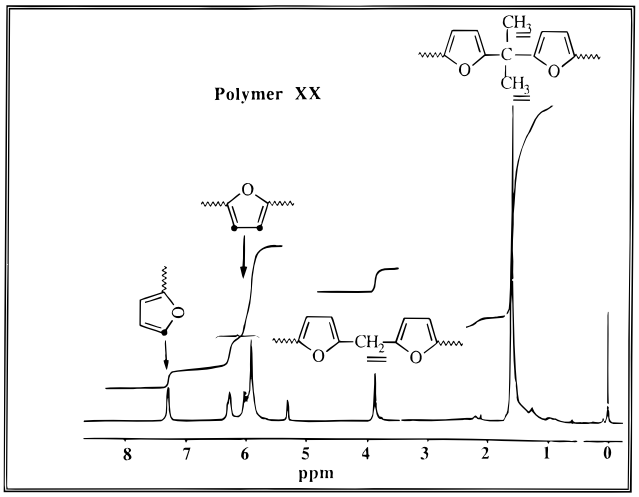

Figure 8. ^{1}H-NMR spectrum (300 MHz) of polymer XX in CD_2Cl_2.

polycondensation. As with FA and its silylated homologue, the reaction of FPS was much slower than that of its alcohol under the same conditions. The FTIR of product XIX thus obtained (Figure 5) showed the same pattern as that of XVIII (Figure 3), except for the absence of carbonyl bands and a weaker OH absorption. The structure of XIX was confirmed by its ^{1}H-NMR spectrum which had the same pattern as that of XVIII (Figure 4), but different end-group/chain-unit intensity ratios, and by its ^{13}C counterpart (Figure 6). The DP_n of XIX, measured by VPO and GPC, again in excellent agreement with that calculated from its ^{1}H-NMR spetrum (Table 4), was now almost double the maximum value reached with FP. The DSC thermogram of XIX showed an endothermic peak at 183 °C corresponding to its melting point. This feature provides further evidence of structural regularity. Moreover, with both monomers, the I_p was close to 2 (see Table 4), as expected from an unperturbed linear polycondensation.

In conclusion, the use of FP and its silylated derivative provided a means to minimize side reactions. With FPS, DPs were higher thanks to the virtual absence of water, which also suppressed the minor ring-opening events.

In order to corroborate the role of hydrogen atoms versus methyl groups attached to the α-carbon of the furanic alcohols, we proceeded to study the mixed structure HMFP in the standard reaction conditions given in Table 4. The polycondensation was slow relative to that of FA, but gave a high yield of a highly viscous product (XX) with a brownish color, much lighter than that of IX and XVII. Its FTIR spectrum (Figure 7), compared with that of HMFP, showed a substantial decrease of the νOH band at 3450 cm^{-1} and the νCH band of monosubstituted furan hetrocycles at 735 cm^{-1}, whereas the band at 767 cm^{-1}, characteristic of 2,5-disubstituted rings, was increased. The ^{1}H-NMR spectrum of XX (Figure 8) showed that this polymer had a branched structure, as indicated by the relative intensities of the relevant peaks (Table 4). Therefore, as with FA and FE1, the linear condensation reactions of HMFP according to Scheme 1 are accompanied by branching mechanisms. This was confirmed by VPO measurements which gave a DP_n value of about 5 compared with only about 2 from the calculation based on the ^{1}H-NMR spectrum (Table 4) for a linear structure.

The "mixed" structure HMFP contained both methyl and hydrogen atoms at the α-carbon. The lighter color of the ensuing polymer suggests that the degree of conjugation induced by the side reactions responsible for the chromophore formation was attenuated, obviously by the lack of reactivity of the dimethylated moieties (as shown with FP), but the same cannot be readily inferred for the extent of branching, although again the previous results with model compounds indicated that no such ramifications are formed with FP. Thus, the CH_2 groups between the furan rings in the HMFP structure obviously plays an important role (directly or indirectly) in promoting branching.

The systems based on TMFP and TFFP showed that there is no condensation reaction with these two compounds irrespective of their concentration and of the

Table 6. Acid-Catalyzed Copolymerization Systems: Conditions and Yields

A−B copolymer no.	A	B	[A]/([A] + [B])	catalyst	[C] × 10^{-2} (mol/L)	T (°C)	yield (%)
XXVI	FA	FAS	0.01	$TiCl_4$	3	25	20
XXVII	FA	FAS	0.05	$TiCl_4$	3	25	25
XXVIII	FA	FAS	0.1	$TiCl_4$	3	25	30
XXIX[a]	FAS	FPS	0.2	$TiCl_4$	3	25	90[b]
XXX[a]	FAS	FPS	0.4	$TiCl_4$	3	25	80[b]
XXXI[a]	FAS	FPS	0.6	$TiCl_4$	3	25	65[b]
XXXII[a]	FAS	FPS	0.8	$TiCl_4$	3	25	25[b]

[a] 2% of FA was added to initiate the reaction. [b] Soluble fraction.

nature of the Lewis acid used, as shown in Table 4. The strong electron-withdrawing effect of the CF_3 group is undoubtedly responsible for this lack of reactivity, as in the case of styrene derivatives for which a methyl substitution increases the nucleophilic character (better aptitude to cationic polymerization) and a trifluoromethyl group produces the inverse effect (better aptitude to anionic initiation).

FE2 showed a very low reactivity in the present context. This is not surprising because the OH group is now in a more aliphatic configuration and its reactivity with the H5 atoms is therefore very considerably reduced. The FTIR and the ^{1}H-NMR spectra of product XXIII suggested the concurrent intervention of reactions both consuming the OH and H5 sites but also destroying the furanic character, probably through ring-opening.

The polymerization of HAF (Table 5) was qualitatively similar to that of FA, but we observed that HAF is so senstive to daylight that it degraded rapidly on the bench. The recent claim[33] that HAF gives a regular polycondensation product is rather surprising.

Finally, the polycondensation of FM was tested in bulk and showed a different behavior compared with that of the other model compounds investigated here. The ^{1}H-NMR spectrum of the ensuing elastomeric polymer (XXV, Table 5) displayed only a decrease of the intensity corresponding to the S-H proton, while the relative intensity of H3, H4, and H5 remained unchanged. It seems therefore that the reaction mechanism leading to this product is totally outside the present context.

Copolymerization Systems. Table 6 gives the copolymerization systems, conditions, and copolymer yields. The first set of three runs (XXVI−XXVIII) relates to the use of a mixture of FA and its silylated derivative. Apart from the rates of polycondensation which were lower, the lower the proportion of FA, the products obtained reflected the same phenomenology as with polymer IX, i.e., branching and color-forming reactions superposed to the OH−H5 condensation. The DPs remained low.

The second set of experiments (XXIX−XXXII) deals with the use of FAS in conjunction with FPS using a small amount of FA to initiate the polycondensation. Here, the behavior of the systems changed considerably as a function of the monomer feed composition as shown in Table 7. Thus, (i) the lower the yield of soluble fraction, the higher the FAS fraction. This trend is explained by a growing tendency to branching which gives a correspondingly growing amount of cross-linked product. (ii) The intensity ratios of the relevant protons in the ^{1}H-NMR spectra of the soluble products (Table 7) indicate that an increasing proportion of FAS in the feed again brings about a corresponding increase in the degree of branching. In particular, the intensity ratio between OH and H5 decreased as FAS increased, which shows that the hydroxy groups find more and more sites other than C5 with which to react. (iii) The deeper the color of these products, the higher the proportion of FAS in the feed going from yellow to very dark brown. These findings confirm that the origin of both branching and color-forming reactions is related, directly or indirectly, to the presence of mobile hydrogen atoms on the carbon attached to the furan ring. In view of this important conclusion, it was decided to investigate further how these labile moieties intervene in the side reactions which convert a hypothetically linear colorless polymer into a black intractable product.

Table 7. M_n, M_w, I_p, DP, and Different Calculations from the ^{1}H-NMR Spectra of Some Copolymers

copolymer no.	VPO[a] M_n	VPO[a] DP_n	Dp_n by NMR $I_{3,4}/2I_5$	Dp_n by NMR $(I_{CH_3}/6 + I_{CH_2}/2)/I_5$	I_{OH}/I_5 integral ratio
XXVII	390	5.0	1.8		0.5 (1)[b]
XXIX			5.0	5.5	0.7 (1)[b]
XXX			4.0	4.5	0.6 (1)[b]
XXXI			3.5	4.0	0.4 (1)[b]
XXXII			3.0	3.5	0.3 (1)[b]

[a] VPO: vapor pressure osmometry. [b] Values in parentheses are theoretical figures based on head-to-tail linear structures.

Hydride-Ion Abstraction from Model Compounds. The structures of the dimeric (BMFM, BMFE, and BMFP) and trimeric (BMFF) models chosen to simulate the furanic alcohols' oligomers bore methyl groups at both ends to avoid unwanted electrophilic reactions on these particularly sensitive C2/C5 positions. What interested us mostly was to have unsubstituted C3 and C4 sites and an aliphatic bridge mimicking the moiety arising from the head-to-tail condensation reactions of the type shown in Scheme 1, i.e., models of the linear structures. Reactions were carried out in methylene chloride at room temperature by mixing the model compound with the hydride-ion abstractor and following thereafter the UV−visible or the ^{1}H-NMR spectra, depending on the concentrations used.

The electronic spectroscopy called upon very low concentrations of reagents. Thus, the reactions between BMFM, BMFE, BMFP, and BMFF, on the one hand, and IDDCA, on the other, were conducted using concentrations around 10^{-4} M for the model and 10^{-3} M for the salt. Neither the model compounds nor the dioxolenium salts used in this work absorbed significantly beyond about 300 nm. The combination BMFM/IDDCA gave rise to a strong peak at 495 nm, as shown in Figure 9, which grew to a maximum intensity within a couple of hours. A similar reaction in which BMFM at around the same concentration was mixed with a 10-fold amount of TAF (λ_{max} = 410−430 nm) gave a similar behavior as shown in Figure 10. This phenomenology suggests that the salts abstracted a hydride ion from BMFM, since both trityl and dioxolenium cations are well-known for their strong affinity for H^-. If a one-to-one interaction and the total consumption of BMFM are assumed, an extinction coefficient of about 55 000 M^{-1} cm^{-1} can be calculated for the product of this reaction from the two experiments. BMFE behaved similarly to BMFM when confronted with IDDCA, TAF, or TAA under the same conditions, in terms of both the reaction rate and the visible spectrum of the product.

Treatment of the solutions showing the peak at 495 nm with a strong Lewis or Brönsted base produced an

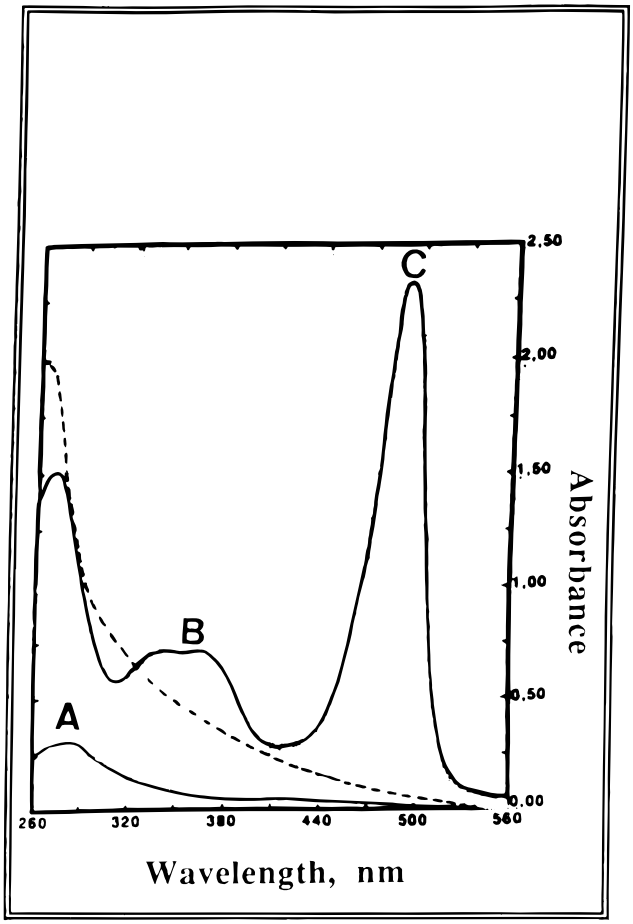

Figure 9. UV−visible spectra of (A) BMFM (10^{-4} M) in CH_2Cl_2; (B) (A) + an equal volume of IDDCA (10^{-3} M) after 2 h; and (C) (B) after neutralization with triethylamine.

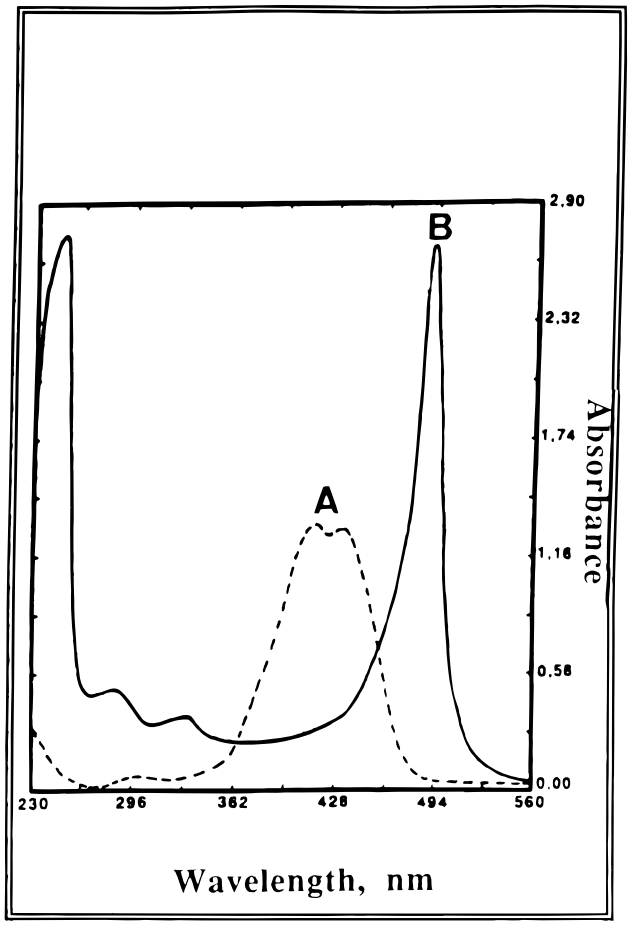

Figure 10. UV−visible spectra of (A) BMFM (10^{-4} M) + an equal volume of TFA (10^{-3} M) in CH_2Cl_2 and (B) (A) after neutralization with triethylamine.

immediate discoloring as shown in Figure 9. Clearly, the colored species formed from the furanic model dimer was a Lewis acid, and most probably a delocalized carbenium ion.

BMFP, on the contrary, gave no reaction with the two hydride-ion abstractors as shown by the fact that the UV−visible spectra did not change within several hours and only reflected the presence of the initial reagents.

The ^{1}H-NMR investigation of these systems involved the same reagents mixed in CD_2Cl_2 at concentrations about 1000 times higher. In these conditions, the strong acidity of the salts used induced side reactions on the furanic models within about 1 h. However, when BMFM and BMFE were submitted to hydride-ion abstraction, the spectra clearly indicated the formation of the neutral dioxolane (from IDDCA) or triphenylmethane (from TAF). With BMFP, no such products were detected.

There is little doubt that the reactions involved in this part of the study consist of a hydride-ion abstraction from the carbon atom joining the two furan rings (Scheme 3). The inertness of BMFP indicates that the H3, the H4, and the methyl hydrogens are not reactive in this context.

The reaction between BMFF and the hydride-ion abstractors was investigated by UV−visible spectroscopy under conditions similar to those employed with the other models as shown in Figure 11. The peak slowly growing at 610 nm reflects a more important conjugation than those obtained in the reactions with the dimeric model compounds. Its extinction coefficient

Scheme 3

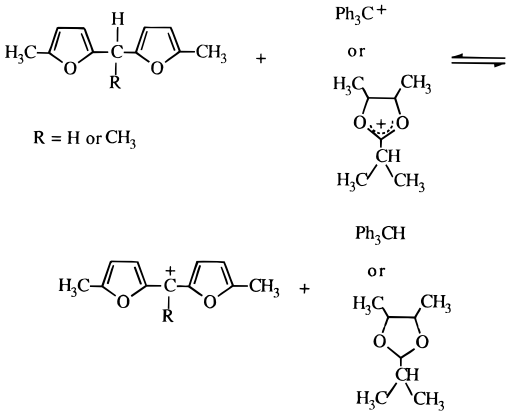

based on complete consumption of BMFF was about double those calculated for the corresponding carbenium ions resulting from BMFM and BMFE. A shoulder around 480 nm also appeared. When the concentration situation was reversed, i.e., the trityl salt was much less than BMFF, the reaction was considerably slower, but went to completion as indicated by the disappearance of the characteristic double absorption of the trityl carbenium ion around 420 nm. The latter experiment also confirmed the presence of a second minor absorption band around 470 nm. The same phenomenology was observed when the trityl salt was replaced by the dioxolenium counterpart.

Neutralization of all these solutions with triethylamine bleached the peaks attributed to carbenium ions

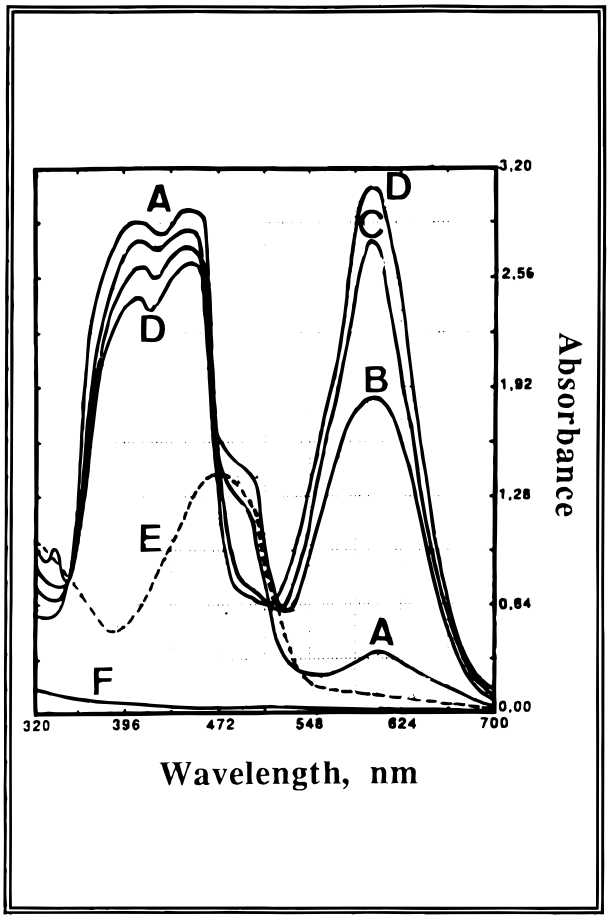

Figure 11. UV−visible spectra of (A) BMFF (10^{-4} M) + an equal volume of TAF (10^{-3} M) in CH_2Cl_2; (B) (A) after 47 min; (C) (A) after 91 min; (D) (A) after 144 min; (E) (D) after neutralization with triethylamine; and (F) BMFF (10^{-4} M) in CH_2Cl_2.

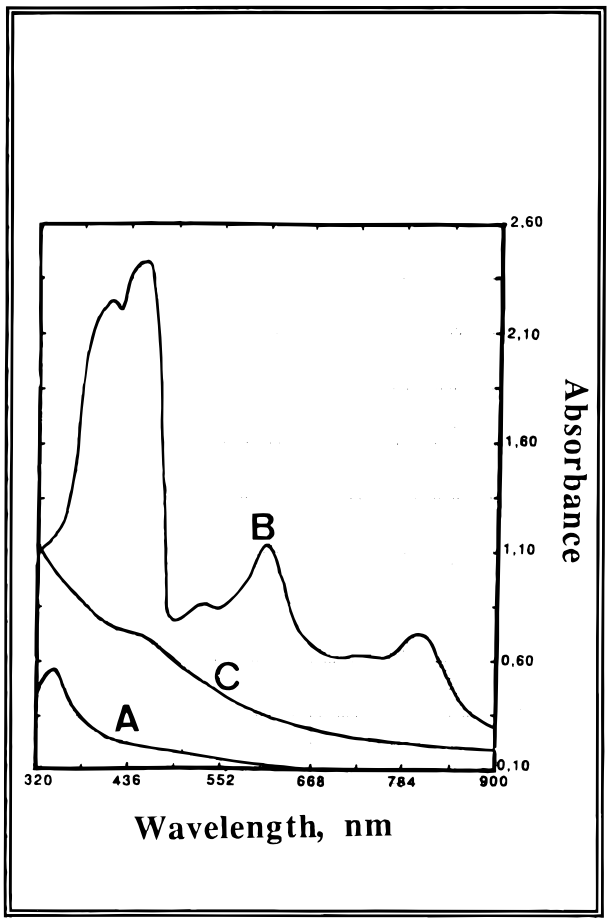

Figure 12. UV−visible spectra of (A) IX (50 mg/L) in CH_2Cl_2; (B) (A) + an equal volume of TAF (10^{-3} M) after 3 h; and (C) (B) after neutralization with triethylamine.

Scheme 4

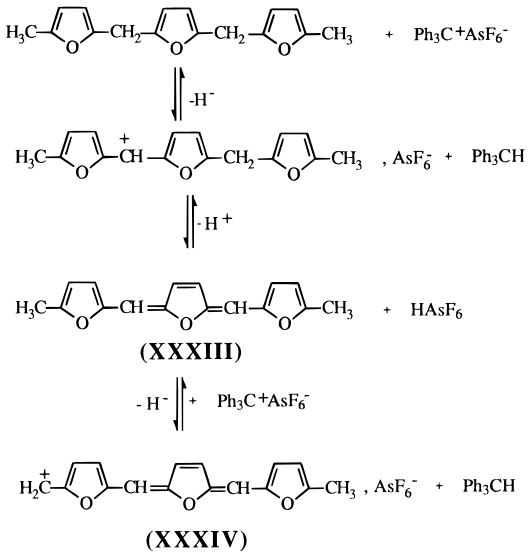

and left a single band around 470 nm which obviously arose from a neutral molecule. The first phase of the mechanism associated with these features is essentially the same as with BMFM and BMFE for the hydride-ion abstraction, but a second phase must now be considered (Scheme 4) which consists of proton expulsion to leave structure XXXIII, which, in turn, can lose a hydride ion to give the highly delocalized carbenium ion XXXIV. The double equilibrium is thus shifted strongly toward the ultimate product XXXIV. When a base is added to these systems, the carbenium ions are eliminated and the neutral product XXXIII, responsible for the peak at 470 nm, is the only absorbing species left.

Treatment of BMFM, BMFE, and BMFF with a 10-fold excess of $SbCl_5$ in methylene chloride at room temperature gave the same qualitative features as those encountered in the corresponding experiments described above. In these systems, the most likely initial reaction is the transfer of an electron from the furanic model to the oxidizing Lewis acid, but the subsequent steps are essentially the same as in the mechanisms proposed with the hydride-ion abtractors.

Hydride-Ion Abstraction from Polymer IX. Typical polymers arising from the acid-catalyzed self-condensation of furfuryl alcohol were submitted to the same treatment as the model compounds, viz., an excess of TAF or IDDFA in CH_2Cl_2 at room temperature. Figure 12 shows the initial spectrum of the polymer with a broad absorption centered around 350 nm and attributed to conjugated sequences also responsible for the dark color of the polymer. After the loss of hydride ions, the spectrum displayed a series of maxima in the visible region apart from the peaks arising from the excess of trityl ions. Neutralization of these carbenium ions led to a product absorbing much more strongly than the original polymer with a maximum around 450 nm and a very broad tail covering the whole of the visible part of the spectrum. Interestingly, a similar reaction with triflic acid produced qualitatively the same phenomenology, but to a much lower extent, because the

Scheme 5

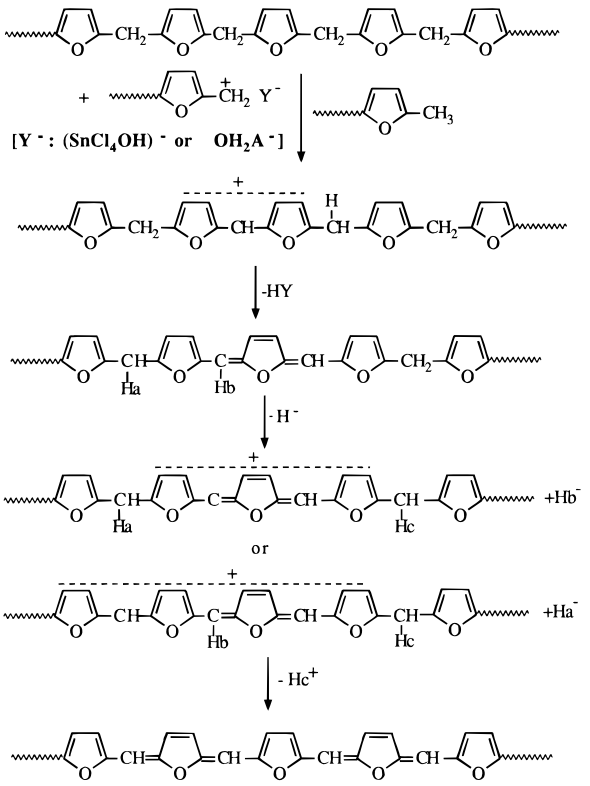

initial step in this case was protonation of the unsaturated sequences.

Mechanism of Color Formation. On the basis of all the results presented above, a mechanism can be proposed which accounts for the progressive coloration of the solutions in which FA is submitted to an acid-catalyzed polycondensation and for the variety of specific observations made in this work (see Scheme 5). The linear condensations, according to Scheme 1, produce oligomers which can undergo hydride-ion exchanges with the protonated chain ends of growing species. This H^- transfer yields methyl-terminated oligomers (see the presence of methyl groups attached to the C2 position of the heterocycle noticed in the NMR spectra of IX) and carbenium ions in which the positive charge is shared by a methyne carbon atom and the two adjacent furan rings. These species are in equilibrium with the corresponding conjugated structure resulting from the loss of a proton. In turn, the latter furanic−dihydrofuranic moiety can lose a hydride ion and eventually give rise to further conjugation as shown in Scheme 5. This sequence of events can occur over and over again, and after each cycle, the degree of conjugation is enhanced. Both the carbenium ions and the corresponding neutral molecules will absorb at growing wavelength as the process advances, as indeed observed by the progressive deepening and red-shifting of the color.

The main culprits of this "side reaction" are the hydrogen atoms of the methylene group separating the furan rings in the oligomers, as shown by the absence of color formation in the polycondensation of FP and the lack of reactivity of BMFP with hydride-ion abstractors. The H3 and H4 positions are obviously *not* involved in the color-forming mechanism. It is worth underlining that in this mechanism the monomer does not necessarily intervene since the H^- and H^+ exchanges can simply take place between oligomeric chains. An analogous situation was encountered in the cationic polymerization of 2-alkenylfurans.[27,28]

The net result of this series of H^- and H^+ tranfers is that for each new conjugated site, i.e., for each new −CH═ moiety formed, there will be a corresponding methyl group at the end of a chain. The fact that the electronic spectrum of IX shows a broad absorption in the visible region suggests that many distinct conjugated sequences are present, each absorbing at a given wavelength. Treatment of these oligomers with hydride-ion abstractors can reinitiate the mechanism of conjugation extension, as witnessed by the corresponding experiments and subsequent spectra. Protonation of the oligomers with triflic acid gives rise to highly delocalized carbenium ions which again can induce a sequence of events similar to that depicted by Scheme 5.

In an attempt to minimize the importance of the color-forming mechanism, we carried out some polycondensations of FA in 4,5-dimethyl-2-isopropyl-1,3-dioxolane instead of methylene chloride. It was thought that this compound would replace the oligomers as a source of hydride ions and thus preserve the unconjugated character of the FA linear macromolecules. Although the phenomenology was slowed down, the improvement was too modest to be be interesting. This shows that the mobility of the H^- attached to a carbon atom linked to two furan rings is extremely high. This is also the case when one considers the ease of abstracting a hydrogen atom in a free radical process, e.g., the fact that poly(vinylfuran) readily cross-links in air by the loss of the tertiary hydrogen atom followed by radical coupling. Moreover, this mobility is equally important in a nucleophilic medium and is observed there as a loss of a proton. The latter phenomenon was encountered in a dramatic fashion when we attempted to synthesize the "ideal" FA polycondensate, viz., poly(2,5-furfuryl), by the reaction of 2,5-dilithiofuran with 2,5-dichloromethylfuran in THF and obtained instead a black insoluble resin, just as with FA plus strong acids. Although we did not pursue this aspect any further, it seems clear that oligomers bearing the expected structures were indeed formed, but that a mechanism complementary to Scheme 5 (initial loss of protons, formation of carbanions, loss of hydride ions, etc.) led to the same type of polyconjugated products.

Origin of Chain Branching. Whereas the direct evidence gathered in the realm of the formation to conjugated sequences leaves no doubt as to the main features of the mechanisms involved, the reactions responsible for the branching and eventually the cross-linking of the FA polycondensates are less easy to pinpoint. What can be readily done is to refute a number of mechanistic proposals given in the past by different authors:

(i) The C3 and C4 positions cannot be held responsible for these side reactions because on the one hand FP gives linear products and on the other hand MFA only dimerizes through a head-to-head condensation, without any products arising from the involvement of the H3 and H4 atoms. Moreover, MFA does not react with MMF under the usual acidic conditions.

(ii) The branching is not caused by products arising from the acid-catalyzed hydrolysis of furan rings. In fact, again FP gives linear products, but also the polycondensation of dry FAC gives branching and finally cross-linking despite the absence of water in the medium and thus of hydrolysis resulting from ring-opening.

(iii) The methylene bridges between furan rings are not the source of branching. In fact, we carried out acid-

Scheme 6

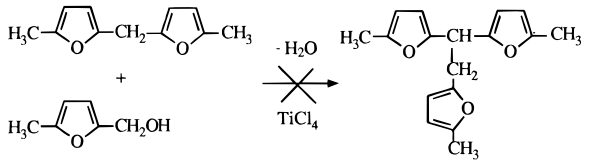

Scheme 7

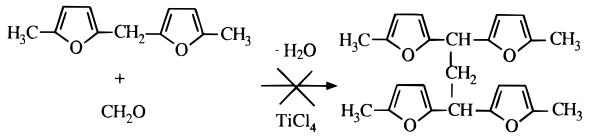

catalyzed reactions between MFA and BMFM to see whether any condensation would take place between the OH group of the alcohol and the CH_2 moiety of the dimeric model compound. No evidence was obtained of any such reaction, and the only product was an increase of BMFM arising from the dimerization of MFA according to Scheme 2. These tests were carried out to confirm the negative evidence already obtained from the very fact that MFA only gives BMFM and *no detectable product* which would originate from their mutual condensation or indeed from the condensation of the formaldehyde generated in situ (Scheme 2) with two methylene groups belonging to two BMFM molecules (Schemes 6 and 7).

It must be emphasized that the branching reactions are *not* sporadic events, but show a very steep increase in rate as soon as oligomers are formed, as indicated by the NMR spectra and by the sudden character of the occurrence of cross-linking. Indeed, the reaction medium tends to go from oligomers with low DPs to insoluble materials, and, to our knowledge, no one has ever reported high molecular weight soluble products from the acid-catalyzed polycondensation of FA, i.e., intermediate situations between short chains and networks. This behavior suggests that the functionality of the oligomers with respect to branching reactions is high, i.e., that the moieties responsible for these events accumulate rapidly in the oligomeric structures. The only reasonable way to rationalize this evidence consists of attributing this growing reactivity toward branching to the unsaturations formed by the recurring mechanism shown in Scheme 5. In other words, branching is conditioned by the occurrence of conjugation, as indeed proved by the absence of ramifications with systems deprived of mobile hydrogen atoms (FP). Therefore, the side reaction leading to a gel can only occur after conjugated structures have appeared in polymers like IX.

The sites associated with conjugation are both the C3 and C4 atoms of the dihydrofuran rings and the exo double bonds attached to these heterocycles. In order to check the reactivity of this type of sites in terms of possible electrophilic substitutions or condensation reactions, we studied the evolution of the ^{1}H-NMR spectrum of the system MFA/3,4-dihydrofuran/$SnCl_4$ in deuterated methylene chloride at room temperature. No reaction other than the self-condensation of MFA was detected; i.e., the presence of dihydrofuran rings did not interfere with the system. An analogous result was obtained when 2,5-dimethoxy-3,4-dihydrofuran was used as a possible source of condensation. The same absence of reactivity was encountered when the corresponding agent was isoprene, showing that the tertiary hydrogen atom in this molecule is not reactive toward MFA. The

Scheme 8

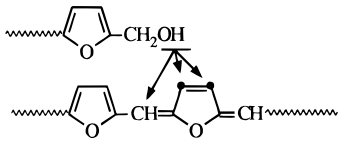

Scheme 9

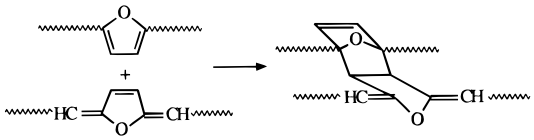

above simulations of sites possibly involved in branching reactions are not conclusive because of the lack of substantial conjugation in the structures chosen with respect to the actual moieties in the FA oligomers, but suggest that a high degree of π-delocalization is perhaps necessary for these important side reactions to occur. In other words, the consumption of primary OH groups through acid-catalyzed condensations other than those in Scheme 1 is not ruled out, but must imply hydrogen atoms in highly conjugated sequences like those depicted in Scheme 5, viz., Scheme 8.

Another mechanism which is compatible with the numerous pieces of evidence obtained in this and previous work consists of envisaging a Diels−Alder reaction between a furan ring (diene) in an oligomeric molecule and a conjugated dihydrofuranic sequence (dienophile) in another oligomer, viz., Scheme 9.

Work is in progress to elucidate these aspects, in particular by setting up model reactions for this type of hypothetical Diels−Alder cycloaddition and by using furan derivatives bearing substituents at C3 and C4 which would slow down such reactions through steric hindrance.

Conclusion

The origin of conjugated sequences in polymers formed by the acid-catalyzed self-condensation of furfuryl alcohol has been proved thanks to the extensive use of model compounds. The branching and cross-linking events which provoke the gelling of these deeply colored materials are subordinate to the formation of the polyconjugations and occur through the interaction of terminal CH_2OH or disubstituted furan rings with non-furanic unsaturations. Most of the puzzle relative to these much studied systems has therefore been unravelled.

References and Notes

(1) Gandini, A. In *Comprehensive Polymer Science, First Supplement*; Aggarwal, S. L., Russo, S., Eds.; Pergamon Press: Oxford, UK, 1992; p 527.
(2) Gandini, A.; Belgacem, M. N. In *The Polymeric Materials Encyclopedia*; Salamone, J., Ed.; CRC Press, in press.
(3) Gandini, A.; Belgacem, M. N. *Prog. Polym. Sci.*, in press.
(4) Mitiakoudis, A.; Gandini, A. *Macromolecules* **1991**, *24*, 830.
(5) Boufi, S.; Belgacem, M. N.; Quillerou, J.; Gandini, A. *Macromolecules* **1993**, *26*, 6706.
(6) Boufi, S.; Gandini, A.; Belgacem, M. N. *Polymer* **1995**, *36*, 1689.
(7) Gandini, A.; Méalares, C. *Trends Polym. Sci.* **1994**, *2*, 127.
(8) McKillip, W. J. *ACS Symp. Ser.* **1989**, *385*, 408.
(9) Schmitt, C. R. *Polym.-Plast. Technol. Eng.* **1974**, *3*, 121.
(10) Gandini, A. *Adv. Polym. Sci.* **1977**, *25*, 47.
(11) Gandini, A. *Encyclopedia of Polymer Science and Engineering*; Mark, H. F., Bikales, N. M., Overberger, C. G., Menges, G., Eds.; Wiley: New York, 1988; Vol. 7, p 454.
(12) Gandini, A. *ACS Symp. Ser.* **1989**, *433*, 195.

(13) Wewerka, E. M.; Longhran, E. D.; Waters, K. L. *J. Appl. Polym. Sci.* **1971**, *15*, 1437.
(14) Wewerka, E. M. *J. Polym. Sci.* **1971**, *A19*, 2703.
(15) Milkovic, J.; Myers, G. E.; Young, R. A. *Cellulose Chem. Technol.* **1979**, *13*, 651.
(16) Conley, R. T.; Metil, I. *J. Appl. Polym. Sci.* **1963**, *7*, 32.
(17) Maciel, G. E.; Chuang, I. S.; Myers, G. E. *Macromolecules* **1984**, *17*, 1087.
(18) Glowinski, S.; Pajak, Z. *Acta Phys. Pol., A* **1978**, *A54*, 411.
(19) Glowinski, S.; Pajak, Z. *Carbon* **1978**, *A54*, 411.
(20) Buchwalter, S. L. *Polym. Prepr.* (*Am. Chem. Soc., Div. Polym. Chem.*) **1987**, *28*, 211.
(21) Buchwalter, S. L. *J. Polym. Sci.* **1985**, *23*, 2797.
(22) Barr, J. B.; Wallon, S. B. *J. Appl. Polym. Sci.* **1971**, *15*, 1079.
(23) Fawcett, A. H.; Dadamba, W. *Makromol. Chem.* **1982**, *183*, 2799.
(24) Gonzales, R.; Martinez, R.; Ortiz, P. *Makromol. Chem.* **1992**, *193*, 1.
(25) Spange, S.; Schütz, H.; Martinez, R. *Makromol. Chem.* **1993**, *194*, 1537.
(26) Dunlop, A. P.; Peters, F. N. *The Furans*; Reinhold Publishing Co.: New York, 1953.
(27) Alvarez, R.; Gandini, A.; Martinez, R. *Makromol. Chem.* **1982**, *183*, 2399.
(28) Gandini, A.; Martinez, R. *Makromol. Chem.* **1983**, *184*, 1189.
(29) Quillerou, J.; Belgacem, M. N.; Gandini, A.; Roux, G.; Rivero, J. *Polym. Bull.* **1989**, *21*, 255.
(30) Belgacem, M. N.; Quillerou, J.; Gandini, A.; Roux, G.; Rivero, J. *Eur. Polym. J.* **1989**, *25*, 1125.
(31) Belgacem, M. N.; Quillerou, J.; Gandini, A. *Eur. Polym. J.* **1993**, *29*, 1217.
(32) Heyns, V. K.; Hauber, R. *Liebigs Ann. Chem.* **1970**, *733*, 159.
(33) Nelson, D. A.; Hallen, R. T. *J. Anal. Appl. Pyrolysis* **1987**, *12*, 11.

MA951522F